Synthesis of some quaternary ammonium gemini surfactants and evaluation of their performance as corrosion inhibitors for carbon steel in oil wells formation water containing sulfide ions

M. A. Migahed [1,], M.M.Shaban[1],A.A.Fadda[2], Tamer Awad Ali[1],N.A. Negm[1]*

[1] *Egyptian Petroleum Research Institute, Nasr City 11727, Cairo, Egypt*

[2] *Chemistry Departments, Faculty of Science Mansoura University, Mansoura, Egypt*

Abstract

Three quaternary ammonium Gemini surfactants were synthesized, characterized, and evaluated as corrosion inhibitors for carbon steel in oil wells formation water containing sulfide ions. The corrosion inhibition efficiency was measured by using electrochemical impedance spectroscopy (EIS) and Potentiodynamic polarization techniques .The data obtained from (EIS) were analyzed to model the corrosion inhibition process through equivalent circuit. The Tafel polarization results indicate that the inhibitors act as mixed type inhibitors. The nature of protective film formed on carbon steel surface was studied using scanning electron microscopy (SEM) and energy dispersive analysis of X-rays (EDX). The effect of molecular structure on the inhibition efficiency was investigated by quantum chemical calculations. It was found that the inhibition efficiency increased with increasing the length of alkyl group attached to the tertiary nitrogen atom. The values of standard adsorption equilibrium constant and free energy of adsorption for the three inhibitors were calculated and discussed. The adsorption of the inhibitor molecules on carbon steel surface was found to follow Langmuir adsorption isotherm.

Keywords:

Gemini cationic surfactants, Carbon steel, Oil wells formation water containing sulfide ions, EIS, Polarization, SEM, Adsorption process.

---

*Corresponding author. Tel.: +20 1006952123.

E-mail address: mohamedatiyya707@hotmail.com (M. A. Migahed).

1. Introduction

Carbon steel is a common constructional material for many industrial units due to its low cost and excellent mechanical properties. However, it suffers from severe attack in service particularly in oil and gas production systems **[1]**. So that, corrosion process plays an important role in the oil field from the economic and safety point of view. Corrosion inhibitors are of great practical importance, being extensively employed in the reduction of metallic waste in engineering materials **[2]**. Corrosion inhibitors can be divided into four types: (i) inorganic inhibitors, (ii) organic inhibitors, (iii) surfactant inhibitors, and (iv) mixed material inhibitors **[3]**. It was reported that the surfactant molecules have many advantages to be used as corrosion inhibitors during oil production such as, high inhibition efficiency, easy production, low price, low toxicity and biodegradable **[4-6]**. It is well known that, Surfactants containing nitrogen, sulfur and oxygen atoms protect the metal surface via adsorption, creating a barrier against corrosive medium. The adsorption bond strength depends on the chemical composition of the metal, nature of corrosive medium, and structure of the inhibitor molecule **[7].** Gemini surfactants are relatively new class of amphiphilic molecules composed of two hydrophilic and two hydrophobic groups linked by a rigid or flexible molecular spacer **[8]**. The efficiency of gemini surfactants as corrosion inhibitors for carbon steel in various corrosive media have been studied **[9-13]**. Quantum chemical calculations have been widely used to study reaction mechanisms and to explain the experimental results as well as to solve chemical ambiguities. Recently, more corrosion publications contained large quantum chemical calculations **[14-17]**. Such calculations are usually used to explore the relationship between the inhibitor molecular properties and its corrosion inhibition efficiency. Formation water **[18]** is naturally exists in oil and gas reservoirs and contains a variety of dissolved organic and inorganic compounds. Formation water is one of the most corrosive environments in oil field operations due to presence of large quantities of dissolved salts such as chloride and sulfate ions in addition to corrosive dissolved gases such as carbon dioxide and hydrogen sulfide.

Sour process streams that contain sulfide ions and/or H_2S gas are extremely corrosive to metallic constructions because it initiates two types of failures: sour corrosion and sulfide-stress cracking (SSC). H_2S penetrates the lattice of some metals, makes them brittle and causes stress corrosion cracking (SCC) failure in particular of high strength steel **[19].** Sulfur and H_2S may occur naturally or may be generated by sulfate reducing bacteria. The importance of the present work arises to protect carbon steel surface which is susceptible to high concentrations of sulfide ions, typically in oil storage tanks and transporting pipelines

as well. Sulfide ions and hydrogen sulfide gas are generated during the metabolism of sulfate reducing bacteria (SRB) that commonly occurs in infected oil storage tanks. Penetrating holes could be formed due to intensive corrosion process causing equipment failures with high economic impact, hence corrosion mitigation programs are commonly executed in oil field production plants to protect carbon steel surface against the attack of sulfide ions meanwhile SRB mitigation programs are executed to control SRB growth.

Iron or carbon steel corrodes in the presence of H_2S to produce FeS as follow **[20- 22]**:

$$Fe + H_2S \rightarrow FeS + H_2 \qquad (1)$$

This work is aimed to synthesis, three novel environmentally friendly quaternary ammonium gemini surfactants and evaluation of their efficiency as corrosion inhibitors for carbon steel in oil wells formation water containing sulfide ions. Also the work is extended to study the relationship between calculated quantum chemical parameters and the experimental inhibition efficiencies for the undertaken inhibitors as calculated from the electrochemical techniques.

2. Experimental

2.1. Chemical composition of X-70 type carbon steel alloy

The working electrodes used in this work were X-70 type carbon steel with the following chemical composition (wt. /wt. %):0.07 C, 0.25 Si, 1.19 Mn, 0.09 P, 0.001S, 0.05 Ni ,0.03Cr, 0.02 Mo, 0.02Cu, 0.001V and the rest is Fe.

2.2. Synthesis of the inhibitors

2.2.1. Synthesis of 3-dimethyl aminopropyl ester of saturated fatty acid

3-Dimethylamino-1-propanol (0.1 mole, 10.32 g) and sodium metal (0.1 mole, 2.31 g) were mixed under nitrogen atmosphere until the evolution of hydrogen bubbles is stopped. Then acid chloride, namely: dodecanoyl chloride (0.1 mole) was added and portion wise in presence of acetone (100 ml) as a solvent. The reaction mixture was refluxed for 6 hours, and then left to cool overnight. The obtained products were recrystallized twice from diethyl ether, and was denoted as E_{11} for dodecanoyl derivative (melting point: E_{11}= 60 ^{o}C, yield: 89%), ***Scheme 1***.

2.2.2. Reaction of Epichlorohydrin and primary amine

Butyl amine, hexylamine, and octylamine (0.5 mole) and 1 mole of epichlorohydrin were refluxed individually in 250 mL round flask for 6 hrs. The reaction mixture was left to cool overnight. The obtained products of dichloro alkylamines were designated as N_4 for butyl derivative, N_6 for hexyl derivative, and N_8 for octyl derivative, ***Scheme 2.***

2.2.3. Quaternization reaction

N, N-dimethyl aminopropyl ester of saturated fatty acid (E_{11}) (0.05 mole) were refluxed for 12 hrs with N_4 or N_6, and N_8 in the presence of acetone (100 ml) as a solvent. The reaction mixture was left to cool and the solvent was removed under vacuum at 50^{o}C. The obtained quaternary ammonium gemini cationic compounds were recrystallized twice from acetone, then washed by diethyl ether and dried at 35^{o}C under vacuum. The compounds from the reaction of $E_{11}$and N_4, N_6, N_8 were designated as: $E_{11}N_4$, $E_{11}N_6$and $E_{11}N_8$, respectively, ***Scheme 3.***

The chemical structure of the synthesized inhibitors was confirmed by elemental analysis, FTIR and ^{1}HNMR spectroscopic techniques.

The elemental analysis was carried out using a Vario Elementar Analyzer instrument (Hanau, Germany).

Infrared (IR) spectra analyses were performed using a Fourier- transform infrared (FTIR) spectrophotometer (ATI Mattson Genesis Series FTIRTM).

^{1}H nuclear magnetic resonance (NMR) spectra analyses were recorded via a Varian Mercury VXR-300 NMR spectrometer at 300 MHz using dimethylsulphoxide (DMSO-d6) as a solvent, and the trimethylsilane spectrum was taken as the zero (0.00 ppm).

2.3. Solution

Corrosive media used in this investigation is formation water obtained from oil well from off shore shukheir petroleum company (OSOCO), Egypt. Complete chemical composition and physical properties of this formation water are shown in **Table 1**. The test solution for this work contains 5000 ppm of sulfide ions in the form of Na_2S.

2.4. Electrochemical measurements

Electrochemical experiments were carried out using Volta lab 80 (Tacussel-Radiometer PGZ402) potentiostat controlled by Voltamaster-4 software. Electrochemical Pyrex glass cell contain carbon steel as working electrode (WE), platinum electrode as counter (CE) and a saturated calomel electrode (SCE) as reference electrode. The working electrode was in the form of a rod from carbon steel embedded by epoxy resin of polytetra fluoro ethylene (PTFE). The exposed electrode area to the corrosive solution was 1 cm^{2}. The working electrode were abraded with a series of emery paper, degreased in ethanol, washed with distilled water and finally dried. The polarization curves were measured at scan rate 2 mVs^{-1}and all the measurements were carried out at 25^{0}C.

EIS measurements were carried out in the frequency range between 100 kHz and 20 mHz using 10 steps per frequency decade at open circuit potential after 3 hours of immersion

time. AC signal with 10 mV amplitude peak to peak was used to perturb the system. EIS diagrams are given in both Nyquist and Bode plots. Each experiment was repeated three times to ensure reproducibility.

2.5. Scanning electron microscopy (SEM)

The surface morphology of the corroded specimens was examined before and after exposure to oil well formation water containing sulfide ions in the absence and presence of a 300 ppm of the synthesized inhibitor ($E_{11}N_8$). Scanning electron microscope (JEOL JSM-5410, Japan) was used for this investigation. The energy of the acceleration beam employed was 30 kV. All micrographs of the corroded specimens were carried out at a magnification power of X = 750.

2.6. Energy dispersive analysis of X-rays (EDX)

EDX system attached with a JEOL JSM-5410 scanning electron microscope was used for elemental analysis or chemical characterization of the film formed on carbon steel surface before and after exposure to oil well formation water containing sulfide ions in the absence and presence of a certain concentration of the synthesized inhibitor ($E_{11}N_8$). The interaction between x-rays and carbon steel surface was recorded as voltage signals through x-ray detector. This information is sent to a pulse processor, which measures the signals and passes them into an analyzer for data analysis and display **[23]**.

2.7. Quantum chemical studies

The molecular structures of $E_{11}N_8$, $E_{11}N_6$ and $E_{11}N_4$ were geometrically optimized by density functional theory (DFT) method using 3-21 G** basis set with Hyperchem 7.5.Quantum chemical parameters such as the energy of the highest occupied molecular orbital (E_{HOMO}) , the energy of the lowest unoccupied molecular orbital (E_{LUMO}), Energy gab ($\Delta E_{L-H} = E_{LUMO} - E_{HOMO}$), dipole moment($\mu$) , Electronegativity (X),Hardness(η),Softness (σ)=1/η ,Chemical potential(π)=−X,and fraction of electron transfer (ΔN) were calculated for the compounds.

3. Results and discussion

3.1. Confirmation of chemical structures of the prepared inhibitors

Chemical composition of the synthesized quaternary ammonium gemini cationic surfactants ($E_{11}N_4$, $E_{11}N_6$ and $E_{11}N_8$) (Scheme 3) was confirmed by elemental analysis: Vario Elementar Analyzer (**Table 2**). The data of elemental analysis confirmed the purity of the synthesized inhibitors. FTIR spectroscopy was performed using Genesis Fourier transformer FTIR™ for $E_{11}N_6$ surfactant as representative sample for the synthesized surfactants. The spectrum showed the following absorption bands: 1169 cm^{-1} correspond to

ether linkage; 1734 cm^{-1} correspond to the ester group; 2857 and 2927 cm^{-1} (CH_3 and CH_2), respectively, and 3387 cm^{-1} correspond to alcohol group and 1072, 655 cm^{-1} for the asymmetric and symmetric stretching N^{+}– C (**Fig.1**). ^{1}HNMR spectroscopy was performed using Varian NMR-300-Mercury 300 MHz spectrometer with TMS as an internal standard. The spectrum of $E_{11}N_6$ in DMSO-d_6 as representative sample for the synthesized surfactants, (**Fig.2**), showed signals at: δ= 0.85 ppm (m, $\boldsymbol{CH_3}(CH_2)_8$), ($\boldsymbol{CH_3}(CH_2)_4$), 1.23 ppm (m, $CH_3\boldsymbol{(CH_2)_8}$, $CH_3\boldsymbol{(CH_2)_4}$), 1.50 ppm (m, $\boldsymbol{CH_2}CH_2C{=}O$), 1.82 ppm (m, $OCH_2\boldsymbol{CH_2}CH_2{}^{+}N$), 2.26 ppm (m, $CH_2\boldsymbol{CH_2}C{=}O$), 2.51 ppm (m, $\boldsymbol{CH_2}N(\boldsymbol{CH_2})\boldsymbol{CH_2}$), 3.17 ppm (s, $^{+}N(\boldsymbol{CH_3})$), 3.47 ppm (m, $^{+}N\boldsymbol{CH_2}CH_2CH_2O$, $CH\boldsymbol{CH_2}{}^{+}N$), 3.65 ppm (m, $OCH_2CH_2\boldsymbol{CH_2}{}^{+}N$), 4.05 ppm (m, OH). The synthesized compounds were completely soluble in water.

3.2. Potentiodynamic polarization measurements

Fig.3 shows the polarization behavior of carbon steel immersed in deep oil wells formation water containing sulfide ions at 25^{o}C with and without various concentrations of $E_{11}N_4$ inhibitor as a representative sample. Electrochemical parameters such as corrosion potential (E_{corr}), cathodic and anodic Tafel slopes (β_c and β_a), polarization resistance (R_p), corrosion current density (i_{corr}) and percentage inhibition efficiency (*IE %*) were calculated and listed in **Table 3** and plotted in Figs. 4, 5 and 6. The values of degree surface coverage (Θ) and the percentage inhibition efficiency (*IE %*) were calculated using the following equation **[24-26]**.

$$\theta = 1 - \frac{i_{corr}}{i^{o}_{corr}} \qquad (2)$$

$$IE\% = \left(1 - \frac{i_{corr}}{i^{o}_{corr}}\right) \times 100 \qquad (3)$$

Where $\boldsymbol{i^{\circ}_{corr}}$ and $\boldsymbol{i_{corr}}$ represent the values of corrosion current density in the absence and presence of inhibitor molecules.

The values of polarization resistance (R_p) were calculated from the well known Stern – Geary equation **[27]**:

$$R_P = \beta_a \beta_c / 2.303\, i_{corr}\, (\beta_a + \beta_c) \quad (4)$$

From the obtained polarization curves, it is clear that the values of corrosion current densities ($\boldsymbol{i_{corr}}$) were decreased with increasing the concentration of inhibitor with respect to the blank curve until critical micelle concentration (CMC) is reached. This behavior confirms a greater increase in the energy barrier of carbon steel dissolution process. Also, it is clear that the values of corrosion potential (E_{corr}) was almost constant. This indicated

that the synthesized inhibitors act as mixed type inhibitor. Also, the slopes of the cathodic and anodic Tafel lines are approximately constant and independent on the inhibitor concentration. This means that, the synthesized inhibitors do effect on the corrosion rate while do not effect on the metal dissolution mechanism. In all inhibitor concentrations; i_{corr} is decreased in the order of $E_{11}N_4 > E_{11}N_6 > E_{11}N_8$.

3.3. Electrochemical impedance spectroscopy

Figs. 7 & 8 show the obtained Nyquist and Bode plots for carbon steel electrode in deep oil wells formation water containing sulfide ions solution in the absence and presence of various concentrations of $E_{11}N_8$ as a representative sample. Nyquist and Bode plots revealed that the impedance response of carbon steel in formation water was significantly changed after the addition of the inhibitor compounds. Both charge transfer resistance (R_t) and hence the inhibition efiiciency (IE%) were found to be increasing by increasing inhibitor concentration as shown in **Figs. 9 and 10**.

EIS spectra of the synthesized inhibitors were analyzed using a suitable equivalent circuit (EC) as shownin **Fig. 11.**Where, R_s is the solution resistance, R_t is the charge transfer resistance, C_{dl} is the electrochemical double layer capacitance, R_f is the film resistance and C_f is the film capacitance. The electrochemical impedance parameters such as charge transfer resistance (R_t), double layer capacitance (C_{dl}), and inhibition efficiency ($IE\%$), were calculated and listed in **Table 4** and plotted in figures 9 and 10**.** Electrochemical double layer capacitance C_{dl} was determined from frequency f_{max} , at which the imaginary component of the impedance ismaximal ($-Z_{max}$) using the following equation **[28,29]**:

$$C_{dl} = (2\pi f_{max} R_t)^{-1} \qquad (5)$$

The values of percentage inhibition efficiency ($IE\%$) were calculated from the values of charge transfer resistance (R_t) according to the following equation **[30]**:

$$IE\% = \left(1 - \frac{R_t}{R_{t(inh)}}\right) \times 100 \qquad (6)$$

Where, $R_{t(inh)}$ and R_t are the values of the charge transfer resistance in the presence and absence of the inhibitor, respectively.

From the impedance data we conclude that the value of R_t increases gradually with increase in concentration of the three synthesized inhibitors and this indicates an increase in the corrosion inhibition efficiency, which is in concord with the potentiodynamic polarization results obtained. The values of R_t in the presence of the inhibitor were always greater than their values in the absence of the inhibitor and C_{dl} value in the presence of the inhibitor was always smaller than its value in the absence of the inhibitor. Hence, the synthesized

compounds act as adsorption inhibitors. The decrease of electrochemical double layer capacitance (C_{dl}) of the tested inhibitors was noticed by increasing their concentration. This may be attributed to the replacement of water molecules in the vicinity of electrode surface by the adsorbed inhibitor molecules which form adherent protective film on the metal surface and lead to decrease in the local dielectric constant of the metal solution interface **[31–33]**. It was found that the values of film resistance (R_f) were increased by increasing the concentration of inhibitors, while (C_f) values were decreased. This data confirm the formation of a good protective film of inhibitors on carbon steel surface. The order of inhibition efficiency was in the following order: $E_{11}N_8$> $E_{11}N_6$> $E_{11}N_4$ that is in good agreement with the order obtained from potentiodynamic polarization measurements.

3.4. Adsorption isotherm

Adsorption isotherms are very important approach to understand the mode of adsorption of surfactant molecules on carbon steel surface. The adsorption process of inhibitor molecules takes place because the interaction energy between the inhibitor and the metal surface is higher than the interaction energy between water molecules and the metal surface **[34]**. The adsorption isotherms provide good information about the interaction between adsorbed inhibitor molecules and carbon steel surface **[35,36].** Two main types of adsorption can take place at electrode surface; physical adsorption and chemical adsorption. To investigate the type of adsorption, C_i/θ is plotted against C_i for the inhibitors as indicated in **Fig. 12**. The experimental results are in good agreement with the Langmuir adsorption isotherm which is represented by the following equation:

$$C_i/\theta = 1/K_{ads.} + C_i \qquad (7)$$

where Θ is the degree of surface coverage, which can be calculated from polarization expermental results, C_i is the molar concentration of the inhibitor and K_{ads} is the standard adsorption equilibrium constant.

The regression coefficients of the fitted curves are around unity (r^2> 0.9765). This reveals that the inhibition tendency of the tested inhibitors is due to the adsorption of these molecules on the metal surface **[37]**. The slope of the isotherm deviates from unity. This deviation may be explained on the basis of interaction between the adsorbed inhibitor molecules on the metal surface by mutual repulsion or attraction **[38, 39]**. K_{ads} values were calculated from intercepts of the straight lines on the C_i/θ axis **[40]**. The standard free energy of adsorption (ΔG°_{ads}) was calculated by the following equation **[41]**:

$$\Delta G^{\circ}_{ads.} = -RTln(55.5\, K_{ads}) \qquad (8)$$

Where R is the universal gas constant (8.314 J mol^{-1} K^{-1}), T is the absolute temperature (K), and the value 55.5 is the molar concentration of water in solution.

The values of ΔG°_{ads} and K_{ads} of $E_{11}N_4$, $E_{11}N_6$ and $E_{11}N_8$ inhibitors were listed in **Table 5**. It is clear that, the large values of K_{ads} indicate a strong adsorption of the synthesized inhibitor on the surface of carbon steel in formation water. The negative sign of ΔG°_{ads} indicates that the inhibitor molecules are spontaneously adsorbed onto the metal surface **[42]**. Generally, the values of ΔG°_{ads} up to -20 kJ mol^{-1}or lower are consistent with the electrostatic interaction between inhibitor and the charged metal surface (physisorption), while those more negative than -40 kJ mol^{-1} involve charge sharing or transfer from the inhibitor molecules to the metal surface to form acoordinate type of bond (chemisorption) **[43-46]**. Regarding the present work, the calculated ΔG°_{ads} values indicated that the adsorption of the prepared quaternary ammonium gemini surfactants on the carbon steel in the deep oil well formation water containing sulfide ions solution is mixed physical and chemical adsorption **[46]**.

3.5. Quantum chemical calculations

Recently quantum chemical calculations are used to study the corrosion inhibition effect of new prepared orangic compounds **[47]**. Quantum chemical calculations are suitabe to make sure whether there is a clear relationship between the molecular structures of the synthesized inhibitors and their inhibition efficiency. Also the quantum chemical calculation can give an idea about the mechanism of the inhibition process. Different quantum chemical parameters were used for the study of inhibition property of an inhibitor, including: the energy of highest occupied molecular orbital (E_{HOMO}), energy of lowest unoccupied molecular orbital (E_{LUMO}), energy gap (ΔE_{L-H}), dipole moment (μ), the electronegativity (X), the ionization potential (I), the electron affinity (A),the global hardness (η), the softness (σ) and the number of transferred electrons from the inhibitor molecules to carbon steel (ΔN). The obtained results are listed in **Table 6** and the frontier molecular orbitals density distributions for the investigated inhibitors are shown in **Fig. 13**.

The ability of inhibitor molecule is related to donate their electrons to the metal surface is associated with the E_{HOMO} values i.e. higher the E_{HOMO} values easier will be the donation of electrons from inhibitor to empty metal d-orbitals. On the other hand, ability of inhibitor molecules to accept the electrons is associated with the E_{LUMO} values i.e. lower its value easier will be the accommodation of additional negative charge by inhibitor molecules,

which is given by filled metal d-orbital. According to the frontier orbital theory, the reaction of reactants mainly occurs on HOMO and LUMO.

Generally, E_{HOMO} and E_{LUMO} have a direct relation to the ionization potential and the electron affinity of an organic molecule. The energy gap, ΔE_{L-H}, is related to the stability index of any inhibitor **[48]**. Thus, lower the ΔE values, higher will be the stability of inhibitor and metal surface interaction **[49]**. It is well known that low absolute values of the energy band gap give good inhibition efficiencies, because the ionization potential will be low due to the energy needed to remove an electron from outer occupied orbital will be low. The dipole moment (μ) provides information about the electronic distribution in molecules and gives a good indication of the molecule polarity. High dipole moment value will favor the enhancement of corrosion inhibition **[50]**.

From **Table 6,** it is clear that E_{HOMO} values are as follows $E_{11}N_8$>$E_{11}N_6$>$E_{11}N_4$, which suggests that electron donation ability of $E_{11}N_8$ is highest and it will adsorb with a greater extent over carbon steel surface, and thus providing highest inhibition efficiency. In the same way E_{LUMO} values are in the order: $E_{11}N_4$ >$E_{11}N_6$>$E_{11}N_8$, lower value of $E_{11}N_8$ indicates its ability to accept electrons and thereby reducing corrosion of carbon steel to a greater extent **[51]**. From **Table 6**, it is evident that μ values are in the order: $E_{11}N_8$ > $E_{11}N_6$ >$E_{11}N_4$, higher value of $E_{11}N_8$ indicates improvement of corrosion inhibition and thereby reducing corrosion of carbon steel to a greater extent. Inspection of the data in **Table 6** revealed that ΔE of $E_{11}N_8$ is lowest, which suggest their adsorptive ability with a greater extent over $E_{11}N_6$ and $E_{11}N_4$. Thus the order of protection of carbon steel in formation water is as follows $E_{11}N_8$> $E_{11}N_6$> $E_{11}N_4$.

Another method to correlate inhibition efficiency with parameters of molecular structure is to calculate the number of transferred electrons from inhibitor to carbon steel surface. The absolute electronegativity (X) and global hardness (η) of the inhibitor molecule are related to electron affinity (A) and ionization potential (I) as follows **[52]**:

$$X = \frac{I+A}{2} \qquad (9)$$

$$\eta = \frac{I-A}{2} \qquad (10)$$

Then **I** and **A** are related to E_{HOMO} and E_{LUMO} as follows **[53]**:

$$I = -E_{HOMO} \qquad (11)$$

$$A = -E_{LUMO} \qquad (12)$$

Thus the number of transferred electrons (ΔN) from inhibitor to carbon steel surface was calculated using the following equation **[54]:**

$$\Delta N = \frac{X_{Fe} - X_{inh}}{2(\eta_{Fe} + \eta_{inh})} \qquad (13)$$

Where X_{Fe} and X_{inh} are the absolute electronegativity of iron and the inhibitor molecule, respectively; η_{Fe} and η_{inh} are the absolute hardness of iron and the inhibitor molecule, respectively. To calculate the fraction of electrons transferred from inhibitors to the iron surface (ΔN) using the theoretical values of X_{Fe} (7 eV mol^{-1}) and η_{Fe} (0 eV mol^{-1}) are used **[55].**

Generally, value of ΔN shows inhibition efficiency resulting from electron donation, and the inhibition efficiency increases with the increase in electron-donating ability to the metal surface. The values of ΔN are less than 3.6, which indicate based on Lukovits's study **[56]** that the inhibition efficiency increases with increasing electron-donating ability at the metal surface.

From **Table 6**, it is evident that ΔN values are in the order: $E_{11}N_8$>$E_{11}N_6$>$E_{11}N_4$, higher value of $E_{11}N_8$ indicates that the electron donation ability of $E_{11}N_8$ is highest and the inhibition efficiency of $E_{11}N_8$ is highest. Based on these calculations, it is expected that the synthesized inhibitors are donor of electrons, and the carbon steel surface is the electron acceptor. Throughout electron donation and acceptance, the synthesized inhibitors bind to the carbon steel surface to form the inhibitive adsorption layer against corrosion.

3.6. Scanning electron microscopy (SEM)

In order to study the morphology of the carbon steel surfaces in contact with formation water, SEM was used. An SEM image of polished carbon steel surface is shown in **Fig. 14(a).** The micrograph shows a characteristic inclusion, which was probably an oxide inclusion **[57]. Fig. 14(b)** shows SEM image of carbon steel surface after immersion in formation water containing sulfide ions for 60 days. SEM image reveals that the surface is highly damaged in absence of the inhibitor. **Fig. 14(c)** shows the image of another carbon steel surface after immersion in formation water containing sulfide ions for the same period in presence of 300 ppm of the synthesized $E_{11}N_8$ inhibitor. From this image it is clear that, the selected inhibitor exhibits a good protective film on carbon steel surface and from scanning electron images reveal that carbon steel surface is quite less damaged in presence of 300 ppm of $E_{11}N_8$ inhibitor however was strongly damaged in absence of the inhibitor. This explains the highest inhibition efficiency of the $E_{11}N_8$ inhibitor at this concentration.

3.7. Energy dispersive analysis of X-rays (EDX)

The protective film formed on carbon steel surface was analyzed using an energy dispersive analysis of X-rays technique (EDX). The EDX spectrum of polished carbon steel sample in **Fig. 15(a)** shows good surface properties, while the EDX spectrum in case of carbon steel sample immersed in oil well formation water containing sulfide ions in the absence of inhibitor molecules for 60 days was failed because it was severely weakened by external corrosion as shown in **Fig. 15(b).**The oxygen signal apparent in **Fig. 15(b)** is due to the carbon steel surface exposed to the formation water in the absence of inhibitor ($E_{11}N_8$). By adding 300 ppm of $E_{11}N_8$ inhibitor, the surface of carbon steel sample was greatly improved and the decrease of iron band was observed due to the formation of a strong protective film of the inhibitor molecules on the surface of carbon steel sample **[58]** as indicated in **Fig. 13 (c).** The protective film formed by inhibitor molecules was strongly adherent to the surface, which leads to a high degree of inhibition efficiency.

The results of both EDX and SEM techniques confirm the formation of a good protective film of the inhibitor molecules on the surface of carbon steel in the presence of 300 ppm of $E_{11}N_8$ inhibitor.

4. Conclusions

The results of the study revealed several conclusions:

(1) Three quaternary ammonium gemini surfactants have been synthesized and characterized by elemental analysis, FTIR and ^{1}H NMR spectroscopy.

(2) The obtained results showed that the synthesized quaternary ammonium gemini surfactants act as effective eco-friendly corrosion inhibitors for carbon steel in oil well formation water containing sulfide ions and can be injected to oil storage tanks to protect it.

(3) The inhibition efficiency increased with increasing concentration of the synthesized inhibitors and the order of inhibition efficiency decreased as follows: $E_{11}N_8 > E_{11}N_6 > E_{11}N_4$.

(4) Tafel polarization curves indicate that the corrosion current density is decreased by addition the inhibitor molecules, while the corrosion potential is slightly changed. Therefore the synthesized quaternary ammonium gemini surfactants can be described as mixed type inhibitors for carbon steel in oil wells formation water containing sulfide ions.

(5) The results of EIS indicate that the value of C_{dl} tends to decrease and both R_{ct} and IE% tends to increase by increasing the inhibitor concentration. This result can be attributed to increase of the thickness of the protective film formed on carbon steel surface.

(6) The adsorption of these inhibitors on the carbon steel surface obeys Langmuir adsorption isotherm. The values of adsorption equilibrium constant suggested that the synthesized inhibitors are strongly adsorbed on the carbon steel surface. The negative sign of the ΔG°_{ads} indicate that the adsorption process is spontaneous .The values of free energy of adsorption indicate that the adsorption is mixed physical and chemical adsorption.

(7) Surface analysis tools such as SEM and EDX indicated that the inhibitor molecules formed a good protective film on the carbon steel surface which isolates the surface from the aggressive environment.

(8) The smaller gap between E_{HOMO} and E_{LUMO} favors the adsorption of the synthesized cationic surfactant on iron surface and enhancement of corrosion inhibition.

(9) The data obtained from the experimental electrochemical techniques are confirmed by theoretical data obtained from quantum chemical calculations.

Acknowledgments

This work has been financially supported by Egyptian Petroleum Research Institute (EPRI) fund. The authors are greatly thanked to EPRI fund and support. Also, great thanks to Dr. E. A. Khamis for her support to provide quantum chemical calculations.

References

[1]A. Ghazoui , A. Zarrouk , N. Benchat , M. El Hezzat , B. Hammouti , A. Guenbour and R. Salghi ,*Der Pharmacia Lettre*,2013, **5**, 247-256.

[2]H. Zarrok , A. Zarrouk, R. Salghi , Y. Ramli , B. Hammouti , S. S. Al-Deyab , E. M. Essassi and H. Oudda ,*Int. J. Electrochem. Sci*., 2012, **7**, 8958-8973.

[3]A.M. Al-Sabagh, H.M. Abd-El-Bary, R.A. El-Ghazawy, M.R. Mishrif andB.M. Hussein, *Egyptian Journal of Petroleum*,2011,**20**, 33-45.

[4] D.N. Singh and A.K. Dey, Corrosion, 1993, **49**, 594-600.

[5] G. Bannerjee and S.N.Malhotra, *Corrosion*, 1992,**48**, 10-15.

[6] S.T. Arab and E.A. Noor,*Corrosion*,1993, **49**, 122-129.

[7]E. Ebenso, N.O. Eddy and A.O. Odiongenyi,*Port. Electrochim. Acta,*2009,**27**, 13-22.

[8]F. M. Mengerand C. A. Littau, *J. Am. Chem. Soc.*, 1991,**113**, 1451-1452.

[9]M. El Achouri, M.R. Infante, F. Izquierdo, S. Kertit, H.M. Gouttaya and B. Nciri,*Corros. Sci.*, 2001, **43**, 19-35.

[10]X.Wang, H.Yang and F. Wang, *Corros. Sci.,*2010, **52**,1268-1276.

[11] M.A. Hegazy, Corros. Sci.,2009,**51** ,2610–2618.

[12] L.-G. Qiu, Y. Wu, Y.-M. Wang and X. Jiang, *Corros. Sci.,*2008,**50**, 576–582.

[13] I.M. Nessim, A. Hamdy, M.M. Osman and M.N. Shalaby,*J. Am. Sci*., 2011,**7**,78.

[14] G. Gece and S. Bilgic, *Corros. Sci.* , 2009, **51** , 1876– 1878.

[15]M.J. Bahrami, S.M.A. Hosseini and P. Pilvar, *Corros. Sci*.,2010,**52**, 2793–2803.

[16]K.R. Ansari, M.A. Quraishi and Ambrish Singh, *Corros. Sci.*,2014,**79**, 5–15.

[17] B.D.Mert, M.E. Mert, G.Kardas and B .Yazıcı,*Corros Sci.*, 2011,**53**,4265–4272.

[18]F.N. Speller, Corrosion Causes and Prevention, McGraw-Hill, New York, 1951.

[19] S. C. Dexter: 'Sea-water corrosion', Vol. 13, 346, 893; 1987, Materials Park, OH, ASM International.

[20] M.A .Migahed, A.M .Al-Sabagh, E.G .Zaki, H.A .Mostafa and A.S .Fouda,*Int. J. Electrochem. Sci.*,2014,**9** ,7693-7711.

[21] M.A. Migahed, A.A. Farag, S.M. Elsaed, R. Kamal, M. Mostafa and H. Abd El-Bary, *Mater. Chem. Phys.*,2011,**125**,125-135.

[22]Y .Zheng, B. Brown and S. Nešić,*Corrosion*,2014,**70** ,351-365.

[23]M.A. Migahed, M.A. Hegazy and A.M. Al-Sabagh,*Corros Sci.*,2012,**61**, 10–18.

[24] ASTM G3-89, Standard practice for conventions applicable to electrochemicalmeasurements in corrosion testing, 1994.

[25]D. Gopi, K. Govindaraju, V. prakash, V. Manivannan and L. Kavitha, *J. Appl. Electrochem.*,2009,**39**,269.

[26]R.A. Prabhu, T.V. Venkatesha, A.V. Shanbhag, G.M. Kulkarni and R.G. Kalkhambkar,*Corros. Sci.*, 2008 ,**50**, 3356–3362.

[27] M. Stern and A.L. Geary, *J. Electrochem. Soc.*,1957 ,**104**,56-63 .

[28]J. Cruz, T. Pandiyan and E.G. Ochoa,*J. Electroanal. Chem*. ,2005,**583**,8-16.

[29]A. P. Yadav,A. Nishikata and T.Tsuru,*Corros. Sci.*,2004,**46**,169-181.

[30] M. Behpour, S.M. Ghoreishi, A. Gandomi-Niasar, N. Soltani and M. Salavati-Niasari, *J. Mater. Sci.*,2009 ,**44**, 2444–2453.

[31]L. Elkadi, B. Mernari, M. Traisnel, F. Bentiss and M. Lagrenée, *Corros. Sci.*,2000,**42**, 703-719.

[32]A.S. Fouda, H.A. Mostafa, F. El-Taib and G.Y. Elewady,*Corros. Sci.*,2005,**47**, 1988-2004.

[33]A. Bonnel, F. Dabosi, C. Deslovis, M. Duprat, M. Keddam and B. Tribollet,*J. Electrochem. Soc.* ,1983, **130**, 753-761.

[34]E. McCafferty, in: H. Leidheiser Jr. (Ed.), Corrosion Control by Coating, *Science Press, Princeton*, 1979, 279-317.

[35] F. Bentiss, M. Traisnel, N. Chaibi, B. Mernari, H. Vezin and M. Lagrenee,*Corros. Sci.*,2002 ,**44**, 2271-2289.

[36] M.B. Valcarce and M. Vazquez, *Mater. Chem. Phys.*,2009, **115**, 313–321.

[37] I.B. Obot and N.O. Obi-Egbedi, *Port. Electrochim. Acta*,2009, **27**, 517–524.

[38] A.S. Fouda, H.A. Mostafa, M.N. MoussaandY.M. Darwish,*Bull. Soc. Chem. France*, 1987, **2**, 261.

[39]A. A. Abdul-Azim, L.A. Shalaby and H. Abbas,*Corros. Sci.*,1974,**14,**21-24.

[40]F. Tang, X. Wang, X. Xu and L. Li, *Colloids Surf. A*,2010, **369**, 101–105.

[41] G. Quartarone, M. Battilana, L. Bonaldo and T. Tortato,*Corros. Sci.*,2008 ,**50**, 3467–3474.

[42] Y.S. Ding, M. Zha, J. Zhang and S.S.Wang, *Colloids Surf. A*,2007,**298**,201–205.

[43] P. Kuteja,J.Vosta,J. Pancir, N. Hackerman,*J.Electrochem.Soc.*,1995,**142**,1847–1850.

[44] M.A. Migahed, R.O. Aly and A.M. Al-Sabagh, *Corros. Sci.*,2004 ,**46**,2503–2516.

[45]P.C. Okafor and Y. Zheng, *Corros. Sci.*, 2009,**51**, 850–859.

[46]M. Behpour, S.M. Ghoreishi, N. Soltani, M. Salavati-Niasari, M. Hamadanian, and A. Gandomi ,*Corros. Sci.*, 2008, **50**, 2172–2181.

[47] G. Gece , *Corros. Sci.*, 2008, **50**, 2981–2992.

[48] D.F.V. Lewis, C. Ioannides and D.V. Parke,*Xenobiotica*,1994,**24**, 401-408.

[49]G. Gao and C. Liang,*Electrochim. Acta*, 2007,**52**, 4554–4559.

[50] J. Zhang, J. Liu, W. Yu, Y. Yan, L. You, and L. Liu, *Corros. Sci.*,2010, **52**,2059–2065.

[51] T. Ghailane, R.A. Balkhmima, R. Ghailane, A. Souizi, R. Touir, M. Ebn Touhami, K. Marakchi and N. Komiha,*Corros. Sci.*,2013,**76**, 317–324.

[52] V.S. Sastri, and J.R. Perumareddi, *Corrosion*,1997,**53**,671–678.

[53]M. Lebrini, M. Lagrenee, M.Traisnel, L. Gengembre, H. Vezin and F. Bentiss , *Appl. Surf. Sci.* ,2007, **253** , 9267–9276.

[54] R.G. Pearson, *Inorg. Chem.*,1988, 27 , 734–740.

[55] S.Martinez, *Mater. Chem. Phys.*,2002,**77**, 97–102.

[56] I. Lukovits, E. Kalman, F.Zucchi, *Corrosion*, 2001,**57**, 3–8.

[57] ASTM E 45-87, Annual Book of ASTM Standard, vol. 11, ASTM, Philadelphia, PA, 1980, p. 125.

[58] M.A. Amin, , *J. Appl. Electrochem.*,2006,**36**, 215-226.

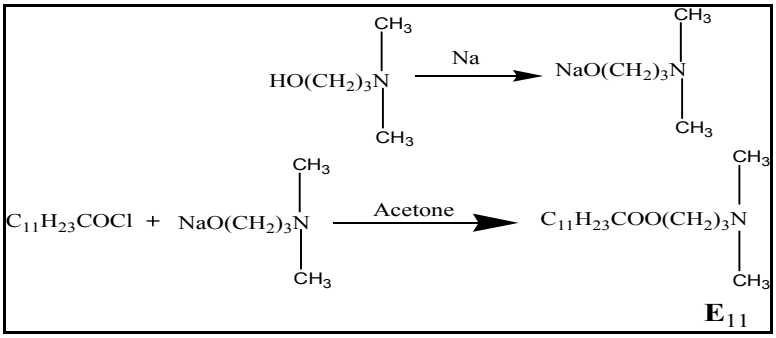

Scheme 1: Synthesis of E_{11}compound.

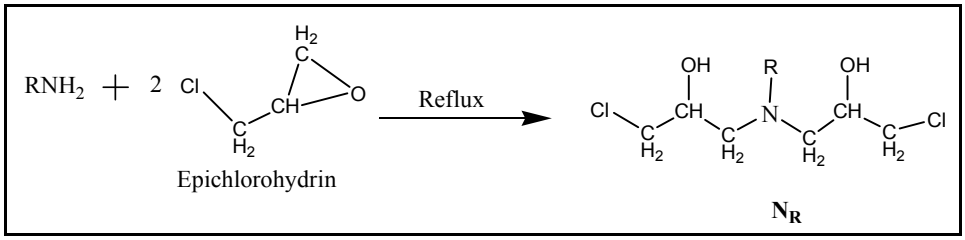

Scheme 2: Synthesis of N_4, N_6, and N_8 compounds; R-C_4H_9, C_6H_{13}, C_8H_{17}.

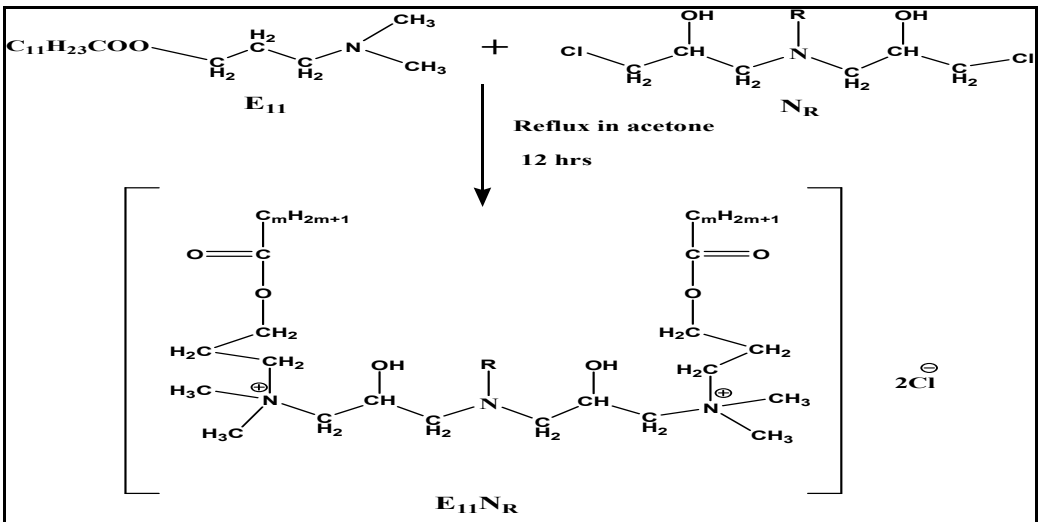

where

R= Butyl amine $CH_3(CH_2)_2CH_2NH2$
Bis{2-hydroxy-3-[3-(dodecanoyloxy)propyldimethylammonio]propyl}
butylamine dichloride ;$E_{11}N_4$

R= Hexyl amine $CH_3(CH_2)_4CH_2NH2$
Bis{2-hydroxy-3-[3-(dodecanoyloxy)propyldimethylammonio]propyl}
hexylamine dichloride ;$E_{11}N_6$

R= Octyl amine $CH_3(CH_2)_6CH_2NH2$
Bis{2-hydroxy-3-[3-(dodecanoyloxy)propyldimethylammonio]propyl}
octylamine dichloride ;$E_{11}N_8$

Scheme 3: Synthesis of the quaternary ammonium gemini cationic surfactants.

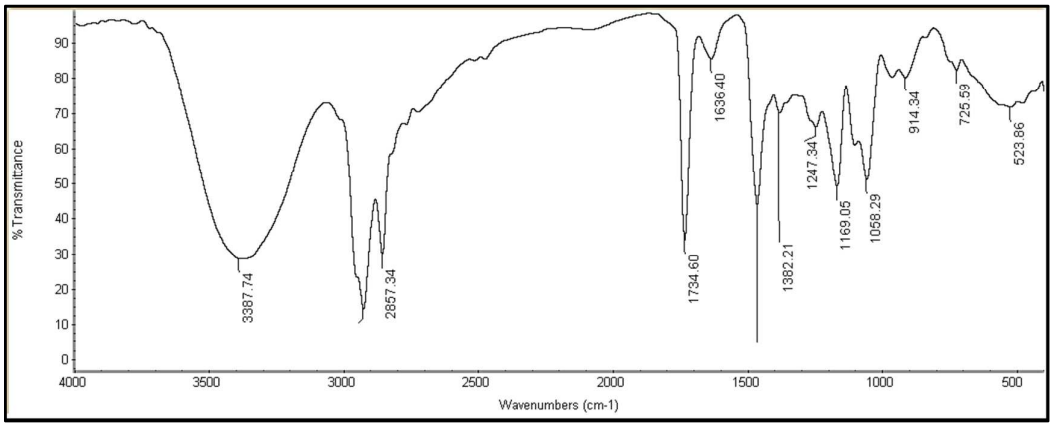

Fig .1.FTIR spectrum of $E_{11}N_6$ quaternary ammonium gemini cationic surfactant.

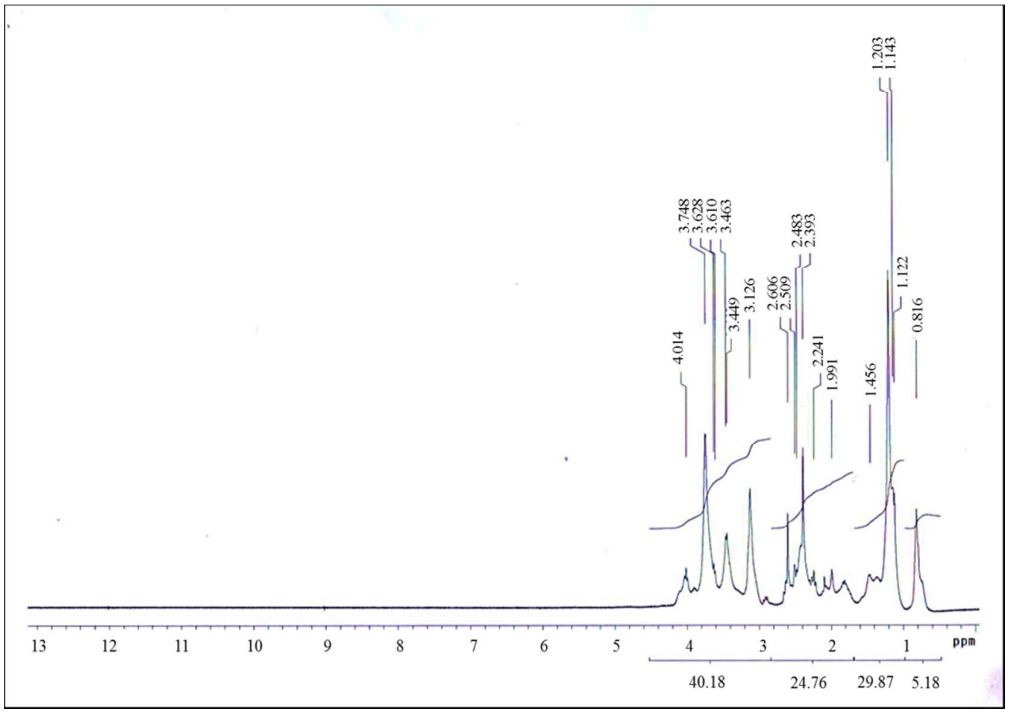

Fig .2. ^{1}**H-NMR** spectrum of $E_{11}N_6$ quaternary ammonium gemini cationic surfactant.

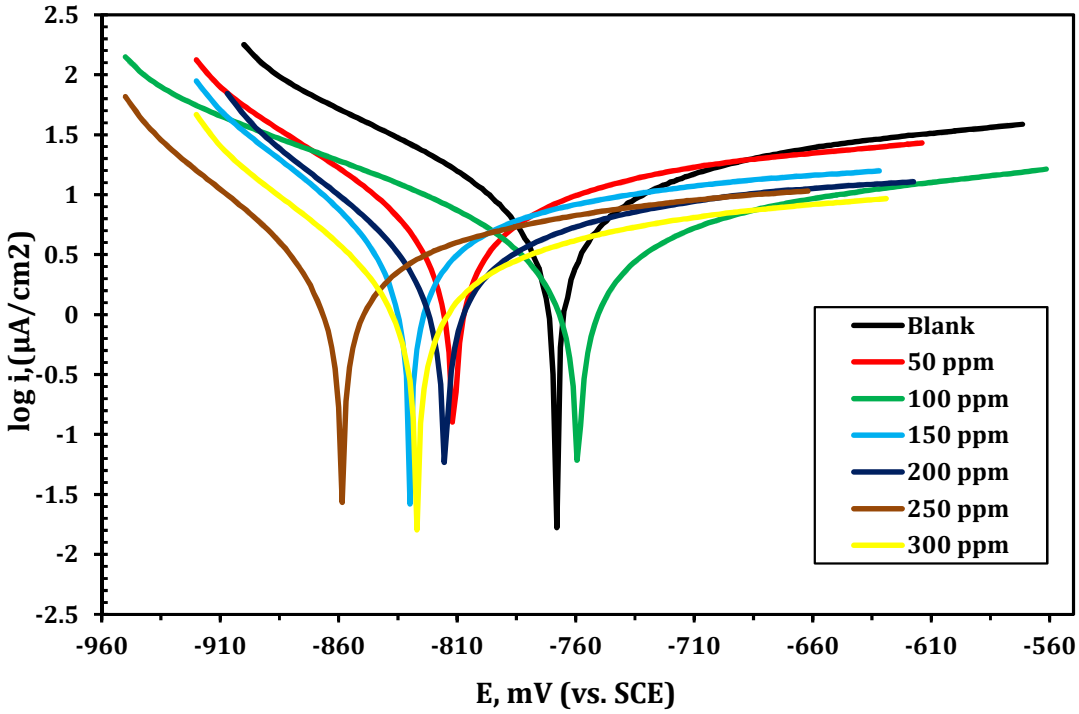

Fig.3. Potentiodynamic polarization of $E_{11}N_8$ for the carbon steel in formation water containing sulfide ions in the absence and presence of various concentrations at 25ºC.

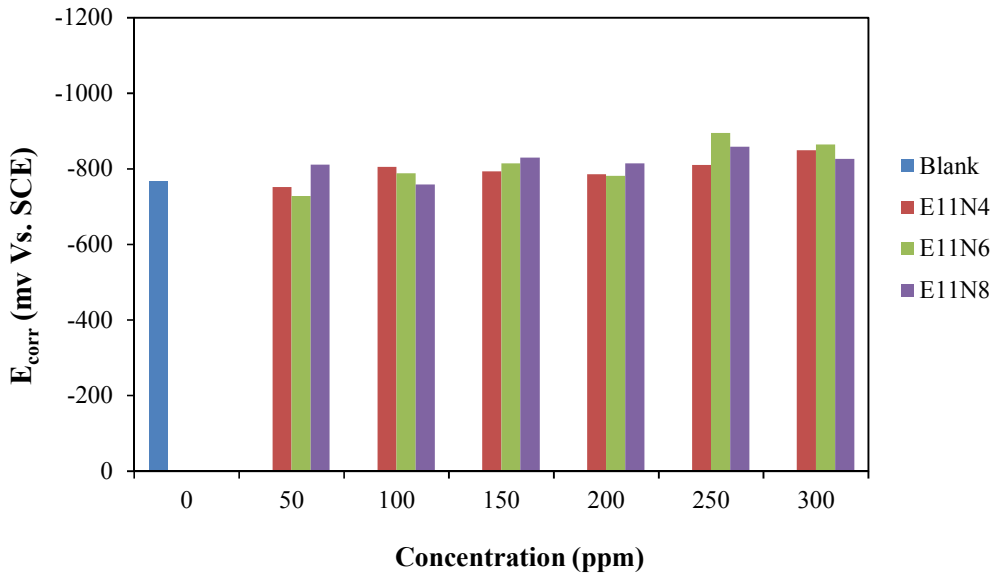

Fig.4. Corrosion potential of $E_{11}N_4$, $E_{11}N_6$ and $E_{11}N_8$ for the carbon steel in formation water containing sulfide ions in the absence and presence of various concentrations at 25ºC as calculated from potentiodynamic polarization technique.

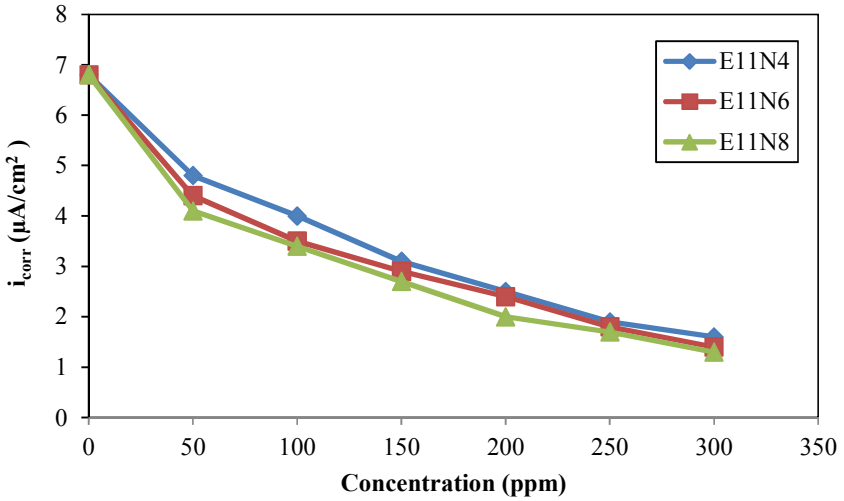

Fig.5. Corrosion current density of $E_{11}N_4$, $E_{11}N_6$ and $E_{11}N_8$ for the carbon steel in formation water containing sulfide ions in the absence and presence of various concentrations at 25ºC as calculated from potentiodynamic polarization technique.

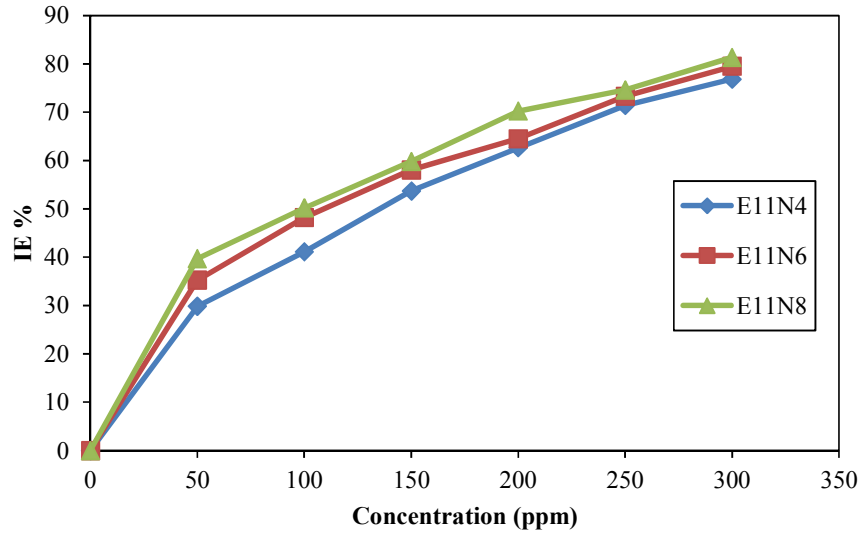

Fig.6. Inhibition efficiency of $E_{11}N_4$, $E_{11}N_6$ and $E_{11}N_8$ for the carbon steel in formation water containing sulfide ions in the absence and presence of various concentrations at 25ºC as calculated from potentiodynamic polarization technique.

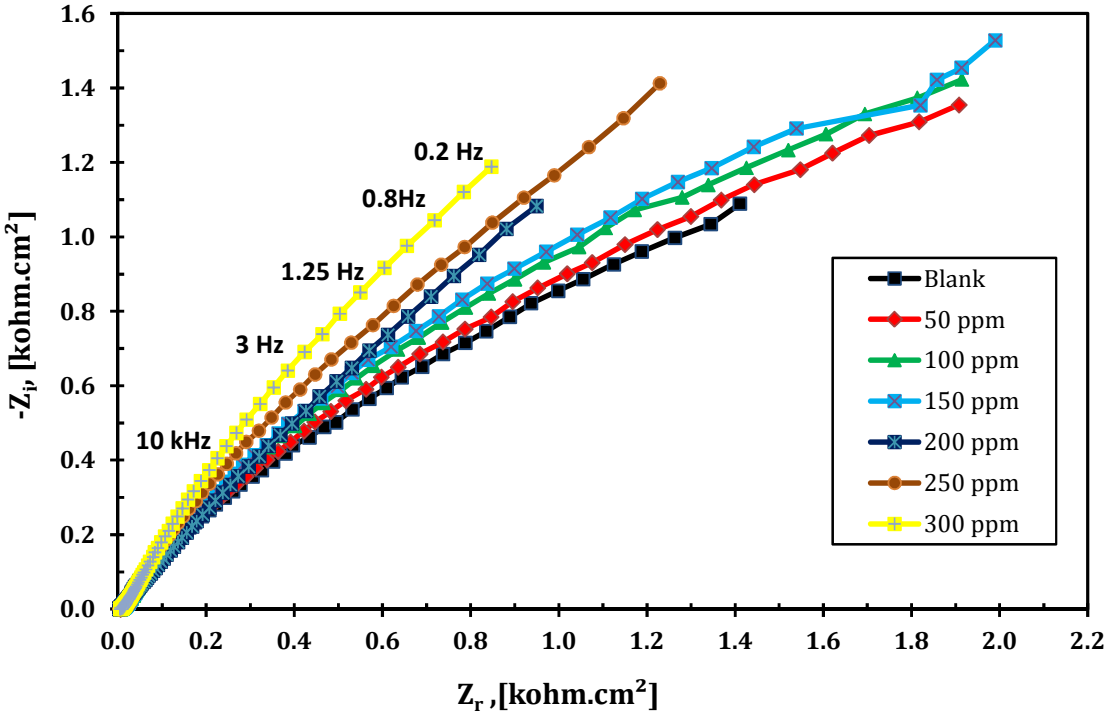

Fig.7. Nyquist plot of $E_{11}N_8$ for the carbon steel in formation water containing sulfide ions in the absence and presence of different concentrations at 25ºC.

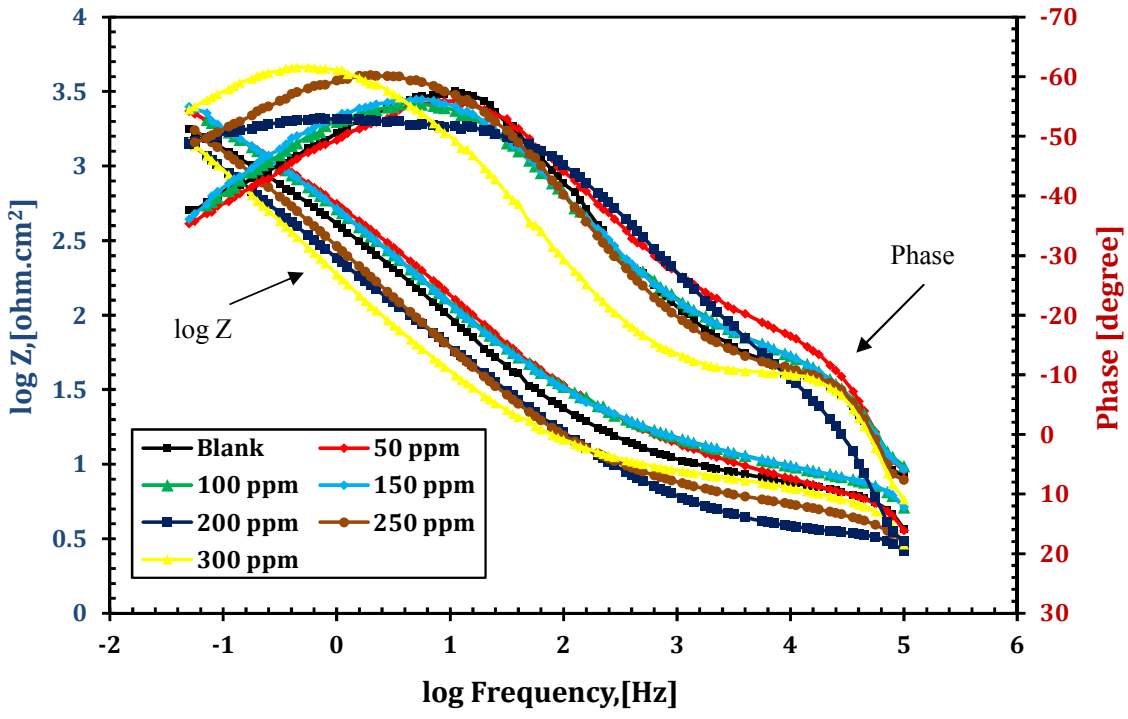

Fig.8. Bode plot of $E_{11}N_8$ for the carbon steel in formation water containing sulfide ions in the absence and presence of different concentrations at 25ºC.

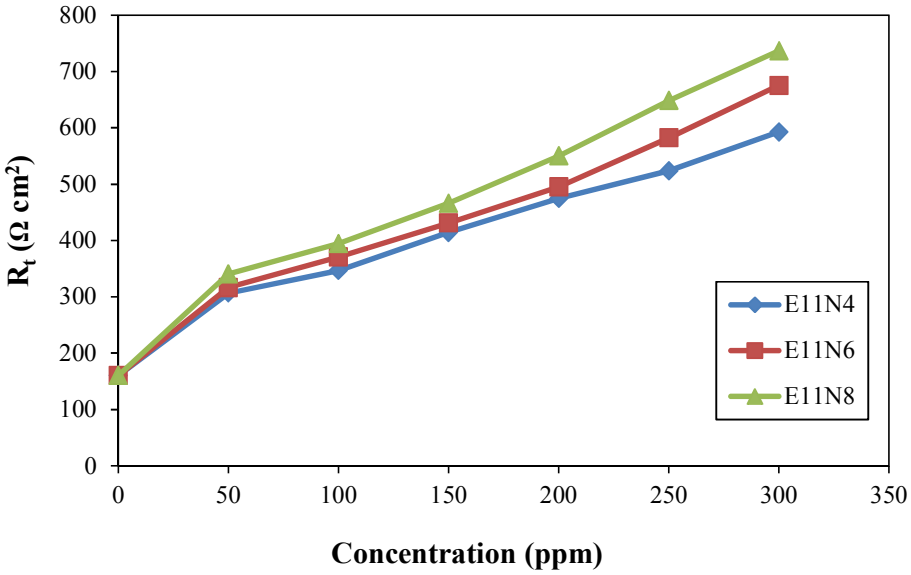

Fig.9. Charge transfer resistence of $E_{11}N_4$, $E_{11}N_6$ and $E_{11}N_8$ for the carbon steel in formation water containing sulfide ions in the absence and presence of various concentrations at 25ºC as calculated from electrochemical impedance spectroscopy.

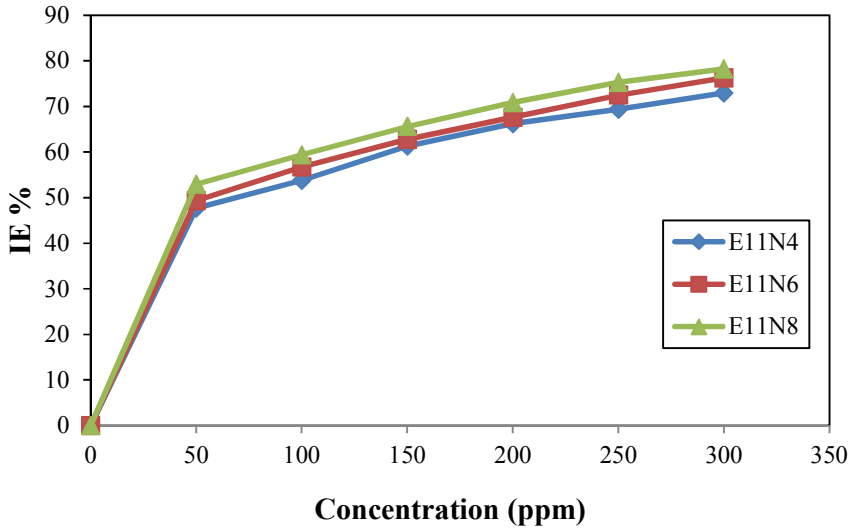

Fig.10. Inhibition efficiency of $E_{11}N_4$, $E_{11}N_6$ and $E_{11}N_8$ for the carbon steel in formation water containing sulfide ions in the absence and presence of various concentrations at 25ºC as calculated from electrochemical impedance spectroscopy.

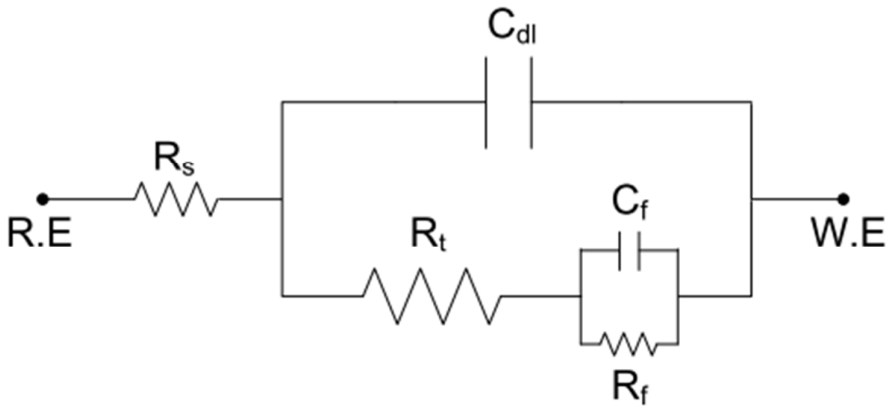

Fig.11: Equivalent circuit used to model impedance data of carbon steel in oil well formation water containing sulfide ions.

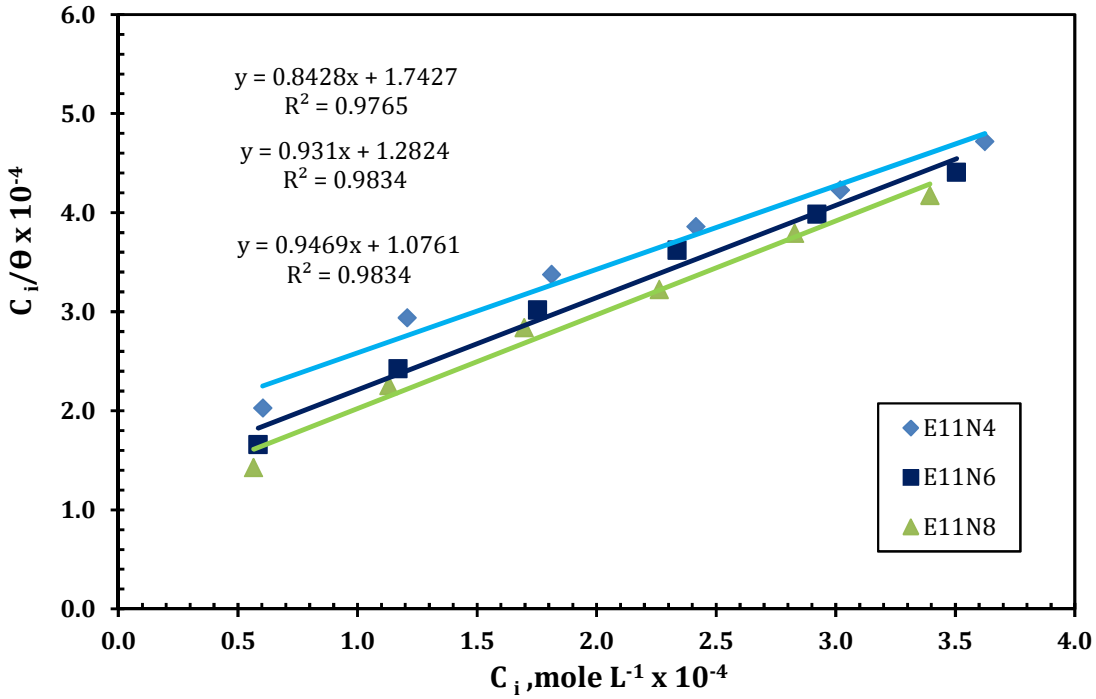

Fig. 12. Langmuir adsorption isotherm of the synthesized inhibitors on the carbon steel surface in formation water at 25ºC.

Inhibitors	HOMO	LUMO
$E_{11}N_4$	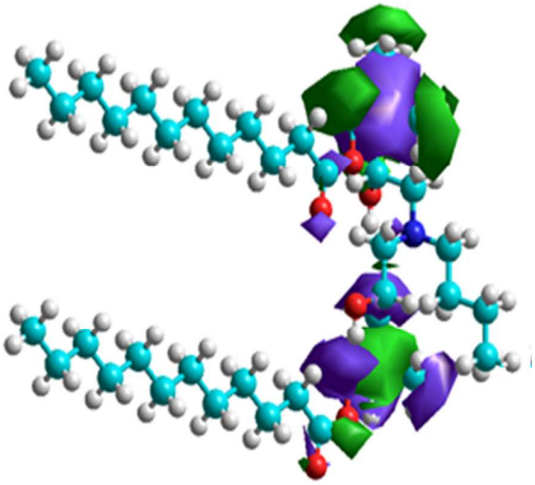	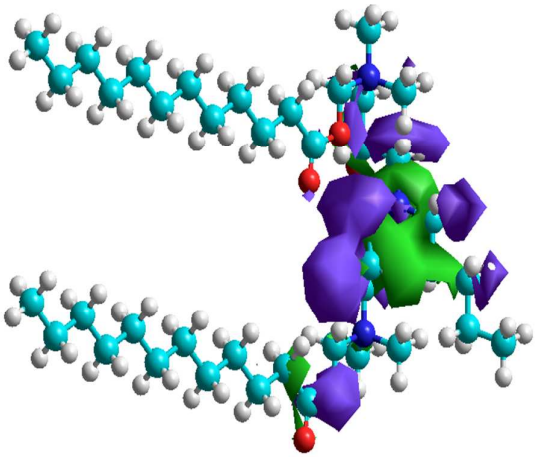
$E_{11}N_6$	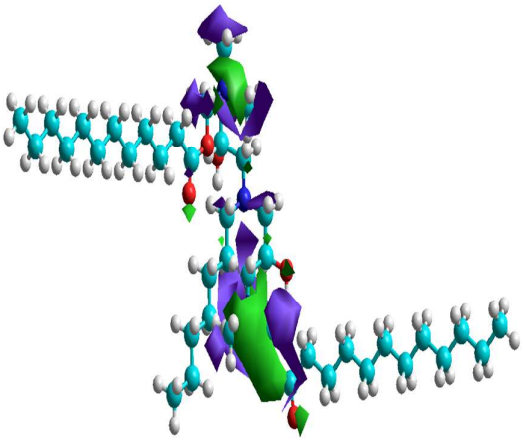	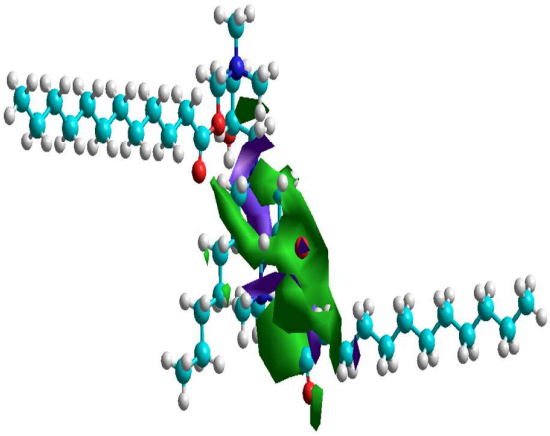
$E_{11}N_8$	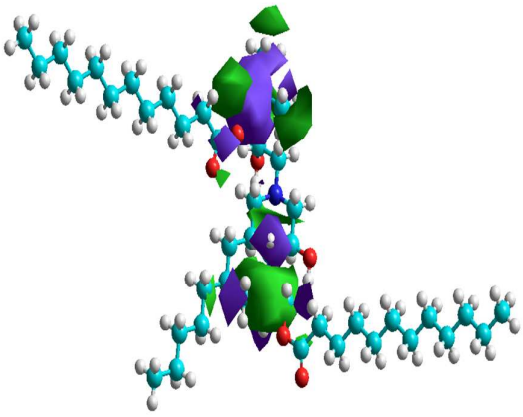	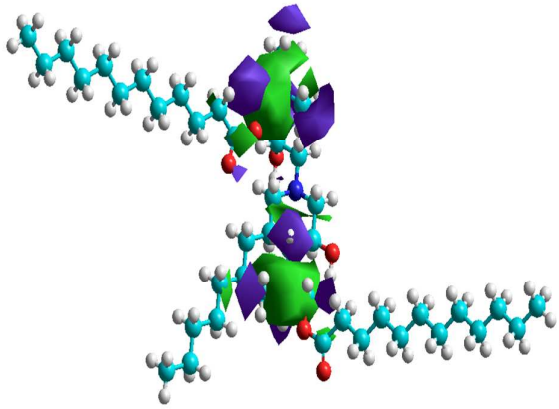

Fig. 13. The frontier molecular orbital density distribution for the investigatedinhibitors.

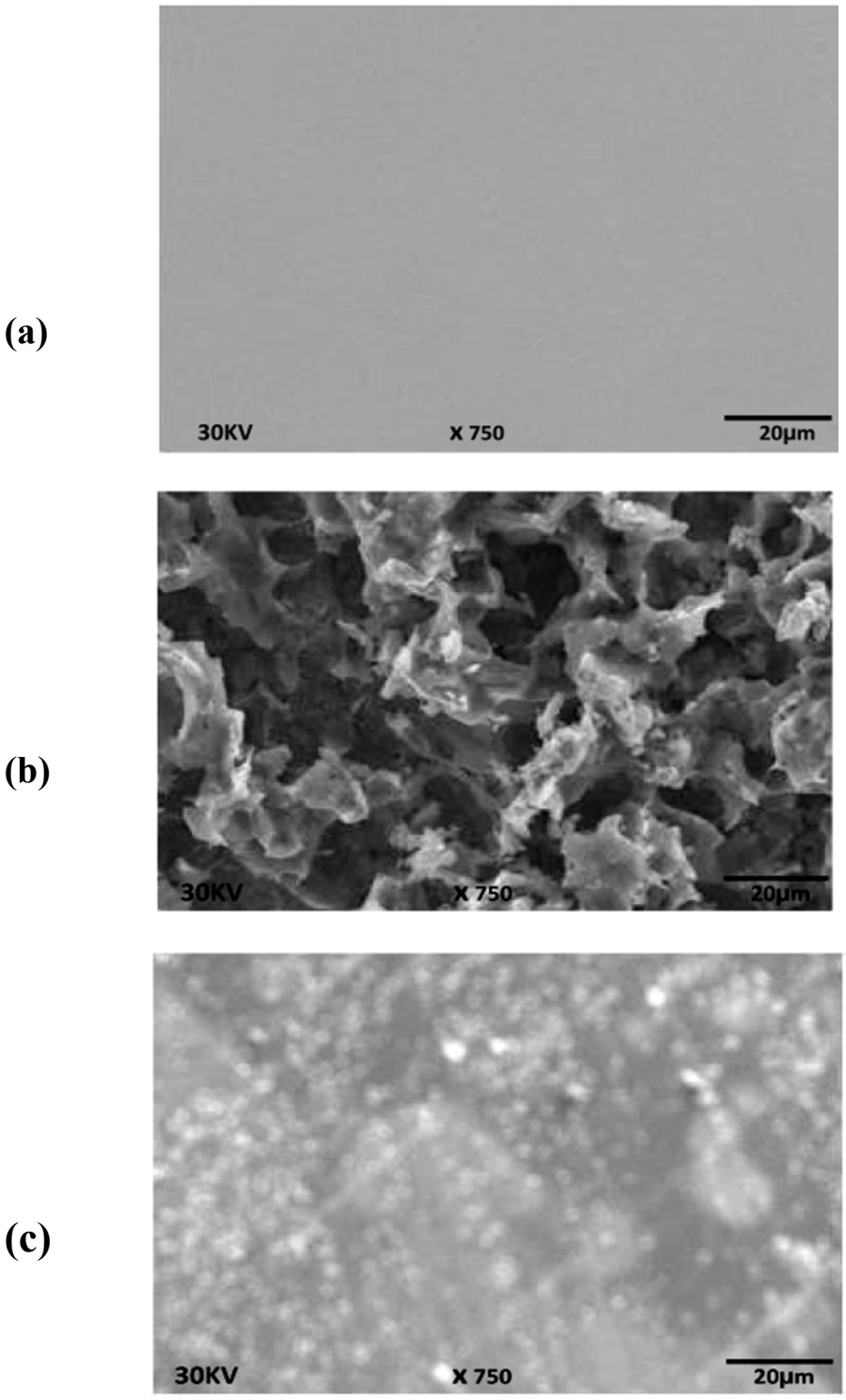

Fig.14. SEM images for the carbon steel surface: (a) polished sample, (b) after immersion in the oil wells formation water containing sulfide ions and (c) after immersion in the oil wells formation water containing sulfide ions in presence of 300 ppm of $E_{11}N_8$ inhibitor.

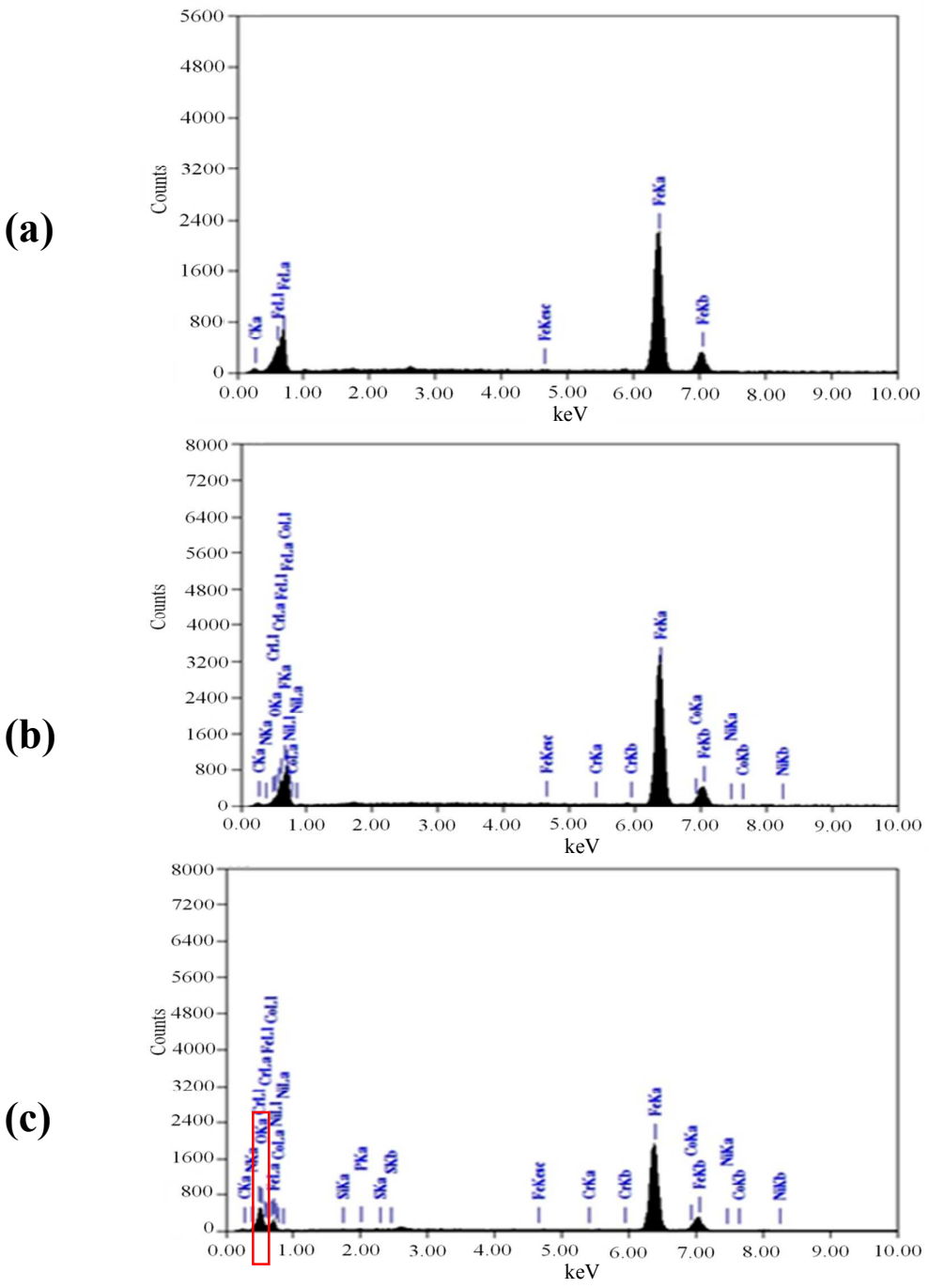

Fig.15. Energy dispersive X-rays analysis (EDX) of carbon steel samples: (a) polished carbon steel surface, (b) after immersion in oil well formation water containing sulfide ions and (c) after immersion in oil well formation water containing sulfide ions in the presence of 300 ppm of $E_{11}N_8$.

Table 1: Chemical composition and physical properties of the deep oil wells formation water containing sulfide ionsused in this work.

Physical properties		
Property	**Unit**	**Value**
Density	g/cm3	1.044
Turbidity	FAU	263
pH		7.66
Specific gravity		1.0050
Salinity as NaCl	ppm (mg/l)	24075
Iron	ppm	3.76
Total alkalinity	ppm	260
Total hardness	ppm	604
Temporary hardness	ppm	260
Permanent hardness	ppm	344
Conductivity	µS/cm	26220
Chemical properties		
Ionic species	**Unit**	**Value**
Sodium & Potassium	ppm	1577
Calcium	ppm	168
Magnesium	ppm	45
Barium	ppm	0.13
Strontium	ppm	8.22
Chlorides	ppm	24720
Sulphate	ppm	577
Bicarbonates	ppm	317
Carbonates	ppm	35
T.D.S	ppm	7000
Barium Sulphate	ppm	0.2
Calcium Carbonate	ppm	260
Strontium	ppm	17
Calcium Sulphate	ppm	217
Magnesium Sulphate	ppm	233
Sod. & Pot. Chlorides	ppm	4448

Table 2: Elemental analysis of the synthesized quaternary ammonium gemini cationic surfactants.

Compound	Structure	Yield, %	MWt (g/mol)	Carbon (C %)		Hydrogen (H %)		Nitrogen (N %)		Chloride (Cl %)	
				Calc.	Found	Calc.	Found	Calc.	Found	Calc.	Found
$E_{11}N_4$	$C_{44}H_{91}N_3O_6Cl_2$	72	828	63.77	63.63	10.99	10.86	5.07	5.00	8.57	8.48
$E_{11}N_6$	$C_{46}H_{95}N_3O_6Cl_2$	81	856	64.48	64.32	11.09	11.01	4.91	4.86	8.29	8.11
$E_{11}N_8$	$C_{48}H_{99}N_3O_6Cl_2$	84	884	65.16	65.05	11.19	11.02	4.75	4.67	8.03	7.89

Table 3: Electrochemical parameters obtained from polarization curves of inhibitors at 25ºC.

Inhibitor	Conc. (ppm)	E_{corr} (mV vs.SCE)	i_{corr} ($\mu A/cm^2$)	corr. rate (μm/Y)	R_P ($k\Omega.cm^2$)	β_c ($mV\ dec^{-1}$)	β_a ($mVdec^{-1}$)	Θ	IE%
Blank	-	-768.2	6.8	79.5	2.6	-104.0	127.0		
$E_{11}N_4$	50	-752.3	4.8	55.8	4.2	-116.8	119.3	0.298	29.85
	100	-805.0	4.0	46.9	5.0	-76.1	116.8	0.411	41.1
	150	-793.6	3.1	36.8	6.2	-79.2	119.5	0.537	53.7
	200	-786.1	2.5	29.7	7.1	-87.3	117.8	0.626	62.64
	250	-810.3	1.9	22.7	9.2	-80.2	114.7	0.714	71.4
	300	-848.9	1.6	18.4	11.3	-75.1	119.9	0.768	76.86
$E_{11}N_6$	50	-728.0	4.4	51.5	4.7	-112.9	112.7	0.352	35.24
	100	-788.6	3.5	41.2	5.6	-81.3	113.4	0.482	48.2
	150	-815.1	2.9	33.3	6.7	-53.4	98.4	0.581	58.05
	200	-781.5	2.4	28.2	7.5	-108.9	119.5	0.645	64.53
	250	-895.4	1.8	21.3	9.8	-57.6	114.6	0.733	73.3
	300	-864.2	1.4	16.3	13.5	-58.8	124.8	0.795	79.49
$E_{11}N_8$	50	-811.5	4.1	47.9	5.2	-79.2	118.2	0.397	39.7
	100	-759.0	3.4	39.6	5.8	-114.5	113.5	0.502	50.2
	150	-829.8	2.7	31.9	6.9	-64.4	129.4	0.598	59.8
	200	-815.1	2.0	23.7	8.5	-65.0	113.0	0.702	70.22
	250	-858.7	1.7	20.2	10.4	-63.5	112.5	0.746	74.61
	300	-826.8	1.3	14.9	16.2	-65.8	122.6	0.813	81.32

Table 4: Electrochemical parameters obtained from electrochemical impedance spectroscopy of inhibitors at 25ºC.

Inhibitor	Conc. (ppm)	**Rs,** (Ω cm^2)	**C_f,** (μF.cm^2)	**n_1**	**R_f** (Ω cm^2)	**C_{dl},** (μF.cm^2)	**n_2**	**R_t,** (Ω cm^2)	**IE%**
Blank	-	4.5	12.4	0.91	12.8	43.9	-0.88	160.4	
$E_{11}N_4$	50	7.2	11.2	0.89	15.7	32.5	0.89	306.5	47.67
	100	6.3	10.1	0.88	16.9	28.5	-0.91	346.7	53.74
	150	5.6	9.3	0.87	17.8	22.1	0.92	414.3	61.28
	200	7.2	8.7	0.89	18.3	18.3	0.93	474.5	66.20
	250	6.8	8.3	0.90	18.7	17.5	0.91	523.6	69.37
	300	6.4	8.1	0.90	19.1	16.2	0.91	592.6	72.93
$E_{11}N_6$	50	6.3	11.3	0.89	21.9	30.8	0.90	316.5	49.32
	100	5.4	10.9	0.89	27.2	26.1	0.91	370.7	56.73
	150	6.3	8.8	0.88	28.3	20.6	0.89	431.1	62.79
	200	7.4	7.8	1.00	29.4	17.5	0.88	495.2	67.61
	250	7.2	7.5	0.99	30.1	15.8	0.91	582.1	72.44
	300	7.1	7.2	0.96	30.5	14.8	0.92	675.4	76.25
$E_{11}N_8$	50	6.1	10.5	0.89	25.7	25.6	0.92	340.4	52.88
	100	6.3	9.7	0.87	29.6	23.2	0.91	394.5	59.34
	150	7.2	8.6	0.91	31.1	15.5	0.88	466.1	65.59
	200	5.9	7.0	0.96	33.4	13.5	0.89	550.0	70.84
	250	6.2	6.9	0.99	35.1	13.0	0.92	648.3	75.26
	300	6.8	6.8	0.91	36.8	12.6	0.91	736.8	78.23

Table 5. Fitting parameters of the adsorption isotherms of the synthesized inhibitors at 25ºC

Inhibitor	Regression coefficient (r^2)	Slope	K_{ads} (M^{-1})	ΔG°_{ads} (kJ mol^{-1})
$E_{11}N_4$	0.9765	0.8428	5738,2	-31.39
$E_{11}N_6$	0.9834	0.931	7797.9	-32.15
$E_{11}N_8$	0.9834	0.9469	9292.8	-32.59

Table 6: Calculated Quantum Chemical Parameters of the Investigated Inhibitors

Inhibitor	E_{HOMO} (eV)	E_{LUMO} (eV)	ΔE(eV)	μ(debye)	I (eV)	A(eV)	X(eV)	π (eV)	η(eV)	σ (eV^{-1})	ΔN
$E_{11}N_4$	-4.03	0.86	4.89	2.16	4.03	-0.86	1.585	-1.585	2.445	0.408998	1.10736
$E_{11}N_6$	-2.10	0.83	2.93	5.45	2.1	-0.83	0.635	-0.635	1.465	0.682594	2.17236
$E_{11}N_8$	-1.43	0.73	2.16	6.42	1.43	-0.73	0.35	-0.35	1.0	0.925926	3.07870